

# Zeolite-encapsulated Cr(III), Fe(III), Ni(II), Zn(II) and Bi(III) salpn complexes as catalysts for the decomposition of H<sub>2</sub>O<sub>2</sub> and oxidation of phenol

M.R. Maurya<sup>a,\*</sup>, S.J.J. Titinchi<sup>a</sup>, S. Chand<sup>b</sup>, I.M. Mishra<sup>b</sup>

<sup>a</sup> Department of Chemistry, Indian Institute of Technology, Roorkee 247667, India

<sup>b</sup> Department of Chemical Engineering, Indian Institute of Technology, Roorkee 247667, India

Received 29 August 2001; accepted 6 November 2001

## Abstract

Cr(III), Fe(III), Bi(III), Ni(II) and Zn(II) complexes of *N,N'*-bis(salicylidene)propane-1,3-diamine (H<sub>2</sub>salpn) encapsulated in Y-zeolite were prepared by flexible ligand method. These complexes were characterized by chemical and thermal analyses, FT-IR and electronic spectral studies and their XRD pattern. The encapsulated materials are active catalysts for the decomposition of hydrogen peroxide and for the oxidation of phenol using H<sub>2</sub>O<sub>2</sub> as oxidant with good selectivity. © 2002 Published by Elsevier Science B.V.

**Keywords:** Encapsulation; Y-zeolite; Spectroscopy; Oxidation of phenol; H<sub>2</sub>O<sub>2</sub> decomposition

## 1. Introduction

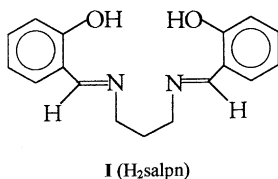
During the last two decades, the isolation, characterization and catalytic activities of metal complexes encapsulated in the cavities of zeolites have been extensively investigated due to their industrial significance [1]. These encapsulated catalysts are often referred to as zeozymes as they behave functionally similar to many enzyme catalysts in some selective oxidation. They possess the advantages of solid heterogeneous catalysts like easy separation, ruggedness, etc., share many advantageous features of homogeneous catalysts and minimize the disadvantages of both [2].

Metal–salen complexes (H<sub>2</sub>salen = *N,N'*-bis(salicylidene)ethane-1,2-diamine) encapsulated in Y-zeolite have been studied for the catalytic activity towards

many reactions such as decomposition of hydrogen peroxide and *tert*-butylhydroperoxide [3–5]; selective epoxidation/oxidation of olefins [6–8] and styrene [9]; oxidation of cyclohexanol [10] and phenol [3–5], and selective hydrogenation [11]. Catalytic activities of other metal encapsulated complexes having ligands *N,N'*-bis(X-salicylidene)ethane-1,2-diamine (X = 5-Cl, 5-Br, 5-nitro) [3–5], and *N,N'*-bis(salicylidene)-hexane-1,6-diamine (H<sub>2</sub>salhexane) [11], acetylacetone bis(anthranilic acid) (H<sub>2</sub>aca) [8], etc. have also been studied. However, only a few studies with complexes of *N,N'*-bis(salicylidene)propane-1,3-diamine (H<sub>2</sub>salpn) have been reported. The [Mn(salpn)] has been used without encapsulation to study its catalytic activity towards the epoxidation of alkenes [8], whereas [Mn(salpn)] encapsulated in Y-zeolite has been used as a catalyst for the oxidation of *p*-xylene [12].

\* Corresponding author.

In the present investigation, we have isolated and characterized Fe(III), Cr(III), Bi(III), Ni(II) and Zn(II) complexes of H<sub>2</sub>salpn (structure I), and tested their catalytic activities for the decomposition of H<sub>2</sub>O<sub>2</sub> and oxidation of phenol. As H<sub>2</sub>salpn has better flexible backbone, it is expected that its insertion into the cavity of the zeolite will be better and hence, formation of metal complexes will be enhanced.



## 2. Experimental

### 2.1. Materials

AR grade metal nitrates and phenol were purchased from Qualigens, India. Salicylaldehyde, 1,3-diaminopropane and hydrogen peroxide (30%) were procured from E-Merck, India. Other reagents and solvents used were also of AR grade. Y-zeolite (Si/Al 10) was obtained from Indian Oil Corporation (R & D), Faridabad, India.

### 2.2. Physical methods and analyses

IR spectra were recorded as KBr pellet on a Perkin-Elmer model 1600 FT-IR spectrophotometer. Electronic spectra were recorded in Nujol on Shimadzu 1601 UV-VIS spectrophotometer by pasting mull of the sample inside one of the cuvette, while keeping another one pasted with Nujol as reference. Thermogravimetric analyses of the pure as well as encapsulated complexes were carried out using TG Stanton Redcroft STA 780 at Scientific Instrumentation Center of the Institute. X-ray diffractograms of solid catalysts were recorded using Philips PW 1140/90 X-ray diffractometer with a Cu-K $\alpha$  target. The metal contents were measured by using Perkin-Elmer model 3100 atomic absorption spectrophotometer. Nucon 5700 chromatograph fitted with FID detector and OV17 (s.s.) column was used to analyze the reaction products.

### 2.3. Preparations

#### 2.3.1. Preparation of ligand (H<sub>2</sub>salpn)

Salicylaldehyde (12.2 g, 0.1 mol) was dissolved in 75 ml of methanol and to this was added a solution of 1,3-diaminopropane (3.75 g, 0.05 mol) in 25 ml of methanol. The reaction mixture thus obtained, was refluxed on a water bath for 1 h. After reducing the volume of the solution to ca. 50 ml, the flask was kept at ambient temperature for 2 h. The yellow shiny plates, which separated, were filtered, washed with cold methanol (2  $\times$  5 ml) and dried. Finally, the ligand was recrystallized from methanol to give pure product, yield 70%; mp 52 °C (lit. 52–54 °C) [13].

#### 2.3.2. Preparation of M-Y (metal exchanged Y-zeolite)

A 0.5 g Na-Y zeolite was suspended in 300 ml distilled water which contained metal nitrate (50 mmol) (nitrates of Fe(III), Cr(III), Bi(III), Ni(II) or Zn(II)). The mixture was then heated while stirring at 90 °C for 24 h. The solid was filtered, washed with hot distilled water till the filtrate was free from any metal ion content and dried for 12 h at 150 °C in air.

#### 2.3.3. Preparation of [M(salpn)]-Y

These encapsulated complexes were prepared by general flexible ligand method. A total of 1 g M-Y and 2.5 g H<sub>2</sub>salpn were mixed in a round bottom flask. The reaction mixture was heated at 100 °C overnight (~14 h) in an oil bath with stirring. The ligand melted at that temperature and acted as a solvent as well as a reactant. The resulting material was taken out and extracted with methanol till the complex was free from unreacted H<sub>2</sub>salpn. The uncomplexed metal ions present in the zeolite were removed by exchanging with aqueous 0.01 M NaCl solution. The resulting solid was then washed with hot distilled water till no precipitation of AgCl on reacting filtrate with AgNO<sub>3</sub> was observed. The coloured (dull colour in case of Bi(III) and Zn(II)) solid was dried at 150 °C for several hours till constant weight was achieved.

### 2.4. Catalytic activity studies

#### 2.4.1. Decomposition of H<sub>2</sub>O<sub>2</sub>

To an aqueous solution of H<sub>2</sub>O<sub>2</sub> (5.5 g, 30%) was added 0.025 g catalyst and the reaction mixture was

stirred for 1 h at ambient temperature ( $\sim 25^\circ\text{C}$ ). At the end of the reaction, the catalyst was separated out. The partly decomposed  $\text{H}_2\text{O}_2$  was diluted to 250 ml in a standard volumetric flask. Ten millilitre of this solution was transferred in a conical flask and titrated with standard  $\text{KMnO}_4$  after addition of 20 ml of 2 M  $\text{H}_2\text{SO}_4$  and 20 ml water.

#### 2.4.2. Oxidation of phenol

A total of phenol (4.7 g),  $\text{H}_2\text{O}_2$  (1.2 g, 30%) and catalyst (0.025 g) was taken in a reaction flask and the reaction mixture was heated at  $80^\circ\text{C}$  for 5 h, while stirring. During this period, the products were analyzed at definite time intervals by withdrawing small aliquots of reaction mixture and injecting into the gas chromatograph.

### 3. Results and discussion

#### 3.1. Syntheses and characterization of catalysts

Synthesis of metal encapsulated complexes in zeolite was carried out by a stepwise method, adopted by Bowers and Dutta [6]. Ratnasamy and co-workers [3] and others [14] described this process as “flexible ligand method”. The metal exchanged M-Y zeolite (M = Ni(II), Zn(II), Fe(III), Cr(III) and Bi(III)) was prepared by exchanging  $\text{Na}^+$  of Na-Y with 0.01 M solution of metal nitrates in aqueous solution. Heating of the M-Y zeolite in excess of ligand at  $100^\circ\text{C}$  for about 20 h effected insertion of the ligand in the cavity followed by complex formation with metal ions. The crude mass was finally purified by soxhlet extraction method in methanol. The remaining uncomplexed metal ions in zeolite were removed by exchanging with aqueous 0.1 M NaCl solution.

An attempt was made to characterize these complexes by comparing their physico-chemical properties with that of the simple complexes prepared by the reaction of  $\text{H}_2\text{salpn}$  with the respective metal nitrates. The formulations of the encapsulated complexes are, thus, based on the respective simple complex. The formula, colour and the percentage of metal content of various catalysts estimated by atomic absorption spectrometer are presented in Table 1.

#### 3.2. Thermal studies

The TGA data of the catalysts along with the weight percentage loss at different steps and their probable assignments are presented in Table 2. The TGA profile of one of the representative catalyst,  $[\text{Ni}(\text{salpn})\cdot 2\text{H}_2\text{O}]\text{-Y}$  is given in Fig. 1. The thermal decomposition of all these catalysts occurs in two to three steps. The endothermic loss in the first step starts shortly after increasing the temperature above  $150^\circ\text{C}$  and continues until the loss of all intrazeolite water. The presence of at least four intrazeolite water molecules has earlier been observed in  $[\text{Cu}(\text{salen})]\text{-Y}$  [10]. We also expect the presence of several water molecules in these encapsulated complexes even after drying them at  $150^\circ\text{C}$  for several hours. As shown in Table 2, exothermic weight loss starts immediately after the first step. In  $[\text{Ni}(\text{salpn})\cdot 2\text{H}_2\text{O}]\text{-Y}$  this loss may be due to two water molecules coordinated to Ni(II) while in  $[\text{Fe}(\text{salpn})(\text{H}_2\text{O})\text{Cl}]$ ,  $[\text{Cr}(\text{salpn})\cdot 2\text{H}_2\text{O}]\text{Cl-Y}$  and  $[\text{Bi}(\text{salpn})\cdot 2\text{H}_2\text{O}]\text{Cl-Y}$ , this is probably due to the loss of water and chloride associated with metal ion. The exothermic loss in the third step, as expected, occurs in a wide temperature range ( $300\text{--}700^\circ\text{C}$ ) and is due to the slow decomposition of the chelating ligand. A very small weight percentage loss indicates the presence of only small amount of metal complex insertion in the cavity of the zeolite. This is in

Table 1  
Chemical composition, physical and analytical data of complexes

S. no.	Catalyst	Metal content (wt.%)	Colour
1	$[\text{Cr}(\text{salpn})\cdot 2\text{H}_2\text{O}]\text{Cl-Y}$	0.166	Pale blue-green
2	$[\text{Fe}(\text{salpn})(\text{H}_2\text{O})\text{Cl}]\text{-Y}$	1.365	Pale brown
3	$[\text{Bi}(\text{salpn})\cdot 2\text{H}_2\text{O}]\text{Cl-Y}$	0.244	White
4	$[\text{Ni}(\text{salpn})\cdot 2\text{H}_2\text{O}]\text{-Y}$	0.445	Off white
5	$[\text{Zn}(\text{salpn})]\text{-Y}$	0.124	Off white

Table 2  
Thermogravimetric data of catalysts

Catalyst	Temperature range (°C)	Loss (wt.%)	Group lost <sup>a</sup>	Type of loss
[Cr(salpn)·2H <sub>2</sub> O]Cl-Y	150–235	16.0	<i>n</i> H <sub>2</sub> O	Endothermic
	235–300	2.0	2H <sub>2</sub> O + Cl	Exothermic
	300–760	7.0	L	Exothermic
[Fe(salpn)(H <sub>2</sub> O)Cl]-Y	150–280	12.0	<i>n</i> H <sub>2</sub> O	Endothermic
	280–370	2.0	H <sub>2</sub> O + Cl	Exothermic
	370–770	7.0	L	Exothermic
[Bi(salpn)·2H <sub>2</sub> O]Cl-Y	150–300	12.0	<i>n</i> H <sub>2</sub> O	Endothermic
	300–380	1.0	2H <sub>2</sub> O + Cl	Exothermic
	380–845	3.6	L	Exothermic
[Ni(salpn)·2H <sub>2</sub> O]-Y	150–215	16.0	<i>n</i> H <sub>2</sub> O	Endothermic
	215–260	0.6	2H <sub>2</sub> O	Exothermic
	260–580	4.4	L	Exothermic
[Zn(salpn)]-Y	150–265	24.0	<i>n</i> H <sub>2</sub> O	Endothermic
	265–595	3.0	L	Exothermic

<sup>a</sup> L stands for salpn<sup>2-</sup>.

agreement with the low percentage of metal content estimated by atomic absorption spectrometer.

### 3.3. XRD studies

The X-ray powder diffractograms (XRD) of Na-Y zeolite, Ni-Y zeolite, [Ni(salpn)·2H<sub>2</sub>O]-Y and simple

complex, [Ni(salpn)·2H<sub>2</sub>O] were recorded to study their crystallinity and to ensure encapsulation. After careful comparison of XRD patterns of Na-Y and Ni-Y, it was observed that, there is one new peak with a *d* value of 1.736 nm in Ni-Y. This peak was also observed in [Ni(salpn)·2H<sub>2</sub>O] and [Ni(salpn)·2H<sub>2</sub>O]-Y at the same position. In addition, the [Ni(salpn)·2H<sub>2</sub>O]-

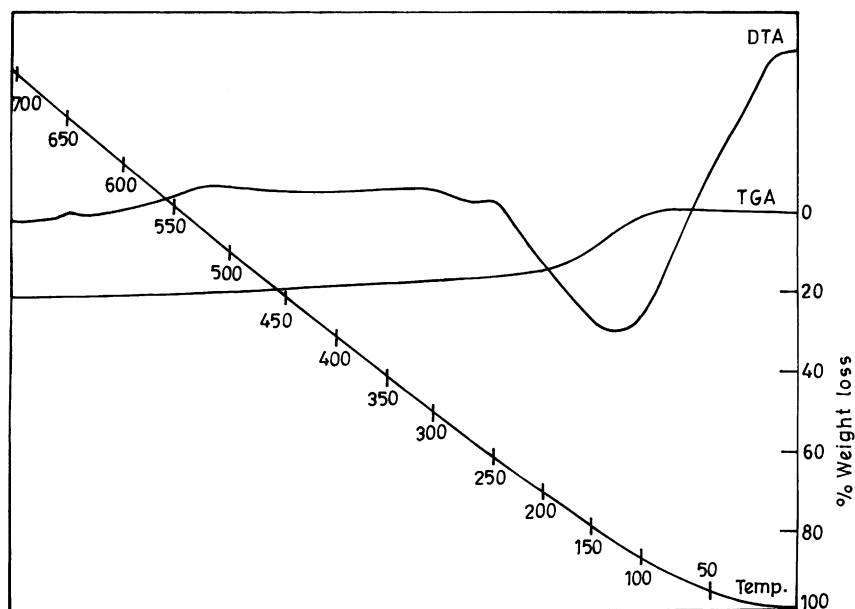


Fig. 1. TGA and DTA profile of [Ni(salpn)·2H<sub>2</sub>O]-Y.

Table 3  
IR ( $\text{cm}^{-1}$ ) and UV–VIS (nm) spectral data of pure and encapsulated complexes

Compound	$\nu(\text{C}=\text{N}), \nu(\text{C}=\text{C})$	$\nu(\text{M}-\text{O})/(\text{M}-\text{N})$	$\lambda_{\text{max}}^{\text{a}}$
$\text{H}_2\text{salpn}$	1580, 1634		404, 316, 225, 216
$[\text{Cr}(\text{salpn})\cdot 2\text{H}_2\text{O}]\text{Cl}-\text{Y}$	1542, 1626	440, 505, 520	581, 377, 270sh, 222
$[\text{Cr}(\text{salpn})\cdot 2\text{H}_2\text{O}]\text{NO}_3$	1545, 1616	418, 447, 532	581, 382, 271, 212
$[\text{Fe}(\text{salpn})(\text{H}_2\text{O})\text{Cl}]-\text{Y}$	1543, 1635	458, 476, 498	470, 325sh, 255, 220
$[\text{Fe}(\text{salpn})(\text{H}_2\text{O})(\text{NO}_3)]$	1552, 1629	448, 470, 507	507, 361, 259
$[\text{Bi}(\text{salpn})\cdot 2\text{H}_2\text{O}]\text{Cl}-\text{Y}$	1560, 1638	431, 447, 518	480, 442, 322
$[\text{Bi}(\text{salpn})\cdot 2\text{H}_2\text{O}]\text{NO}_3$	1550, 1635	447, 518	373, 271, 212
$[\text{Ni}(\text{salpn})\cdot 2\text{H}_2\text{O}]-\text{Y}$	1523, 1639	444, 506	341sh, 260
$[\text{Ni}(\text{salpn})\cdot 2\text{H}_2\text{O}]$	1546, 1632	468, 502	402, 340, 309, 257, 240
$[\text{Zn}(\text{salpn})]-\text{Y}$	1540, 1641	442, 515	373, 272
$[\text{Zn}(\text{salpn})]$	1540, 1627	418, 442, 515	383sh, 352, 320, 260, 238

<sup>a</sup> Sh: shoulder.

Y exhibits one new signal with a  $d$  value of 8.269 nm, which is a part of the ligand as this signal was also observed in  $[\text{Ni}(\text{salpn})\cdot 2\text{H}_2\text{O}]$  but not observed in Na-Y or Ni-Y. This information clearly indicates the insertion of  $[\text{Ni}(\text{salpn})\cdot 2\text{H}_2\text{O}]$  in the cavities of the zeolite. Very low intensity of other peaks made it difficult to distinguish them from the other peaks in the XRD pattern of the encapsulated zeolite.

### 3.4. IR spectral study

A partial list of the IR spectral data of ligand and encapsulated complexes along with their respective simple complexes are presented in Table 3. The intensity of the encapsulated complexes are though, weak due to low concentration of the complex in zeolite, the IR spectra of encapsulated complexes are essentially similar to that of the free metal complexes. However, a significant change in some important bands from free ligand has been noticed. For example, free ligand exhibits  $\nu(\text{C}=\text{N})$  stretch at  $1580\text{ cm}^{-1}$ . In complexes, this band shifts to lower frequency and appears at  $1523\text{--}1560\text{ cm}^{-1}$ , indicating the coordination of azomethine nitrogen to the metal. Appearance of two to three bands in the low frequency region (between  $418$  and  $532\text{ cm}^{-1}$ ) indicates the coordination of phenolic oxygen in addition to azomethine nitrogen. The presence of several bands of medium intensity in  $2700\text{--}2900\text{ cm}^{-1}$  region indicate the existence of ethylene group of the amine residue of the ligand. Thus, IR data indicates the encapsulation of the complexes in the zeolite cavity.

All metal complexes encapsulated zeolites exhibit band around  $1140, 1035, 960, 780$  and  $740\text{ cm}^{-1}$  due to zeolite framework. No significant broadening or shift of the structure-sensitive zeolite vibrations at  $1130\text{ cm}^{-1}$  (due to the asymmetric T–O stretch) on encapsulation of metal complexes indicates that there is no significant expansion of the zeolite cavities or dealumination during the encapsulation process. This further indicates that, the structure of metal complexes fit nicely within the cavity of the zeolite.

### 3.5. Electronic spectral studies

The electronic spectral data of the catalysts are presented in Table 3. Fig. 2 represents the electronic spectra of  $[\text{Cr}(\text{salpn})\cdot 2\text{H}_2\text{O}]\text{Cl}-\text{Y}$  along with the neat  $[\text{Cr}(\text{salpn})\cdot 2\text{H}_2\text{O}]\text{NO}_3$ . Appearance of three bands at  $581, 378$  and  $260\text{ nm}$  in neat as well as in encapsulated complexes, indicate the existence of the same coordination environment around Cr(III) in both complexes. These data nicely compare with the reported value for  $[\text{Cr}(\text{H}_2\text{O})_6]^{3+}$  where these bands appear at  $574.7, 405$  and  $270\text{ nm}$  [15]. Accordingly, these bands are assigned as  ${}^4\text{A}_{2g}(\text{F}) \rightarrow {}^4\text{T}_{2g}(\text{F})$  ( $\nu_1$ ),  ${}^4\text{A}_{2g}(\text{F}) \rightarrow {}^4\text{T}_{1g}(\text{F})$  ( $\nu_2$ ) and  ${}^4\text{A}_{2g}(\text{F}) \rightarrow {}^4\text{T}_{1g}(\text{P})$  ( $\nu_3$ ) transitions, respectively, in an octahedral field. The absorption spectrum of  $[\text{Ni}(\text{salpn})\cdot 2\text{H}_2\text{O}]-\text{Y}$  exhibits only one band at  $314\text{ nm}$  which is clearly due to  ${}^3\text{A}_{2g} \rightarrow {}^3\text{T}_{1g}(\text{P})$  ( $\nu_3$ ) transition as majority of complexes exhibits  $\nu_3$  band in this region [16]. Iron complex,  $[\text{Fe}(\text{salpn})(\text{H}_2\text{O})\text{Cl}]-\text{Y}$  exhibits one d–d band at  $470\text{ nm}$  and three ligand bands.

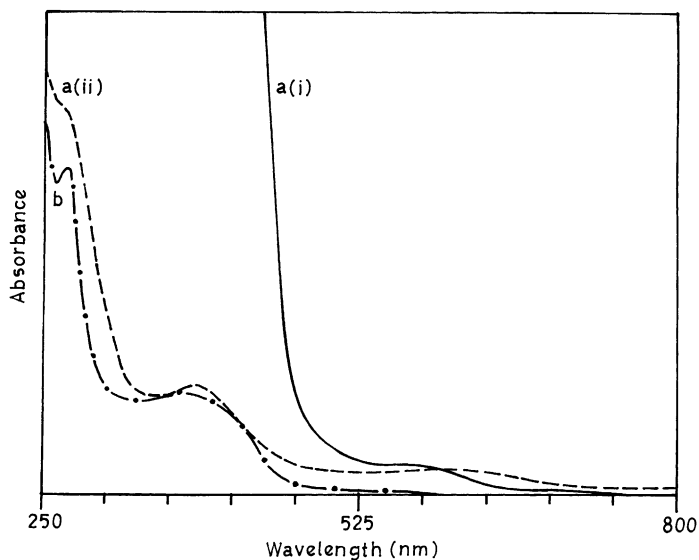


Fig. 2. Electronic spectra of  $[\text{Cr}(\text{salpn})\cdot 2\text{H}_2\text{O}]\text{NO}_3$  [a(i) (—), sample with concentrate paste; a(ii) (---), sample with dilute paste] and  $[\text{Cr}(\text{salpn})\cdot 2\text{H}_2\text{O}]\text{Cl}\cdot\text{Y}$ , b(— · — · —).

### 3.6. Catalytic activity

#### 3.6.1. Decomposition of $\text{H}_2\text{O}_2$

All metal complexes encapsulated in Y-zeolite matrix were tested for their catalytic activities towards the decomposition of  $\text{H}_2\text{O}_2$ . The catalytic activities were observed at different reaction times. Table 4 shows results of the activities of these catalysts as a function of time (0–2 h). It is clear from the data that the decomposition of  $\text{H}_2\text{O}_2$  up to 1 h is relatively slow (3.58–6.42%) in all cases except with the catalyst  $[\text{Zn}(\text{salpn})]\cdot\text{Y}$  which showed a significantly increased decomposition of  $\text{H}_2\text{O}_2$  (~16.4%). The percentage of decomposition of  $\text{H}_2\text{O}_2$  after 2 h has shown different

trends. The turn over frequency (TOF) calculated for the decomposition of  $\text{H}_2\text{O}_2$  after 1 and 2 h is presented in Table 4. For the catalyst  $[\text{Zn}(\text{salpn})]\cdot\text{Y}$ , there is a small or negligible increase in further decomposition, though, there is considerable decrease in TOF after 2 h. Catalysts  $[\text{Cr}(\text{salpn})]\cdot\text{Y}$  and  $[\text{Ni}(\text{salpn})]\cdot\text{Y}$  record two-fold increase in the percentage of decomposition after 2 h in comparison to the observed value within 1 h. On the other hand,  $[\text{Fe}(\text{salpn})]\cdot\text{Y}$  and  $[\text{Bi}(\text{salpn})]\cdot\text{Y}$  show a significant increase of 5–7 times of the corresponding value within 1 h. The TOF values increased by three and two times, respectively in these catalysts. These results, thus, indicate that catalysts  $[\text{Fe}(\text{salpn})]\cdot\text{Y}$  and  $[\text{Bi}(\text{salpn})]\cdot\text{Y}$  require a

Table 4  
Percentage decomposition of  $\text{H}_2\text{O}_2$  after one and two hours at ambient temperature

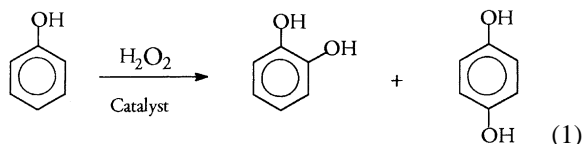
Catalyst	Percentage of $\text{H}_2\text{O}_2$ reacted (1 h)	TOF ( $\text{h}^{-1}$ ) <sup>a</sup>	Percentage of $\text{H}_2\text{O}_2$ reacted (2 h)	TOF ( $\text{h}^{-1}$ ) <sup>a</sup>
$[\text{Cr}(\text{salpn})]\cdot\text{Y}$	5.88	48.80	14.84	52.90
$[\text{Fe}(\text{salpn})]\cdot\text{Y}$	6.20	47.14	45.69	137.47
$[\text{Bi}(\text{salpn})]\cdot\text{Y}$	6.42	77.08	32.10	168.55
$[\text{Ni}(\text{salpn})]\cdot\text{Y}$	3.58	28.68	7.41	26.89
$[\text{Zn}(\text{salpn})]\cdot\text{Y}$	16.36	133.76	17.05	52.65

<sup>a</sup> TOF: turn over frequency—moles of substrate converted per mole of metal (in the solid catalyst) per hour.

relatively longer contact time to attain the maximum equilibrium, while others attain such equilibrium in much shorter time. However, other complexes seemed to be much effective for the decomposition of  $\text{H}_2\text{O}_2$ . The catalytic activities of the catalysts towards the decomposition of  $\text{H}_2\text{O}_2$  after 2 h reaction time were, in the order: Fe(III) (45.7%) > Bi(III) (32.1%) > Zn(II) (17.5%) > Cr(III) (14.84%) > Ni(II) (7.4%).

### 3.6.2. Oxidation of phenol

The catalytic oxidation of phenol using  $\text{H}_2\text{O}_2$  as oxidant was studied as a function of time. Two major products, catechol and hydroquinone as shown by Eq. (1) were identified from the reaction mixture.



To understand the efficiency of the catalysts, the percentage of phenol conversion, the percentage of formation of catechol and hydroquinone were plotted as a function of time, separately and are presented in Figs. 3–5. The results summarized in Fig. 3 indicate that conversion of phenol increases with time in all cases, but acquires steady state at different times. The maximum conversion of about 23% was observed with catalyst [Fe(salpn)]-Y after a period

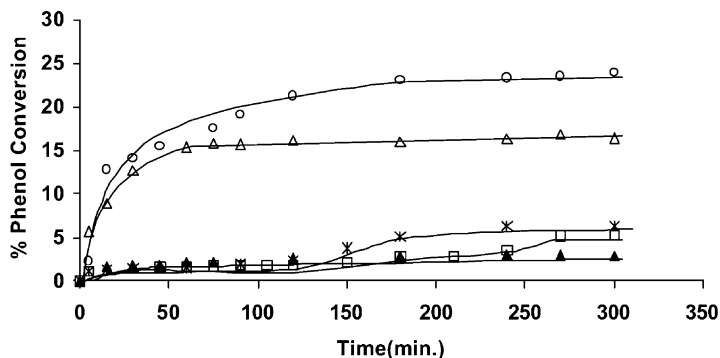


Fig. 3. The percentage of phenol conversion: [Fe(salpn)]-Y (○); [Cr(salpn)]-Y (△); [Bi(salpn)]-Y (\*); [Zn(salpn)]-Y (□) and [Ni(salpn)]-Y (▲).

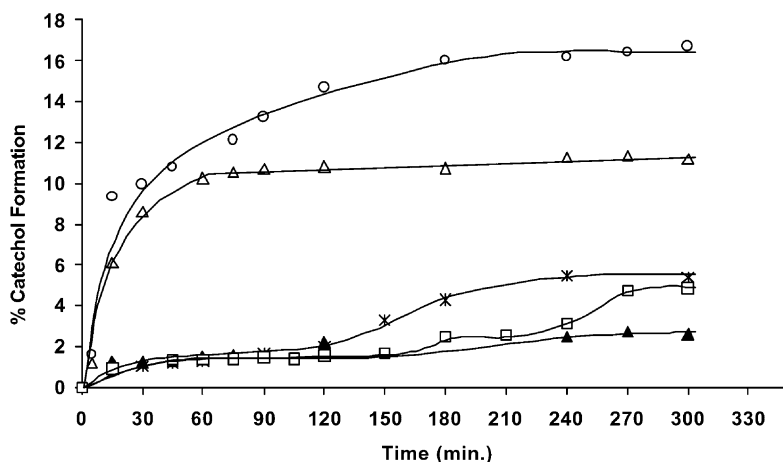


Fig. 4. The percentage of catechol formation: [Fe(salpn)]-Y (○); [Cr(salpn)]-Y (△); [Bi(salpn)]-Y (\*); [Zn(salpn)]-Y (□) and [Ni(salpn)]-Y (▲).

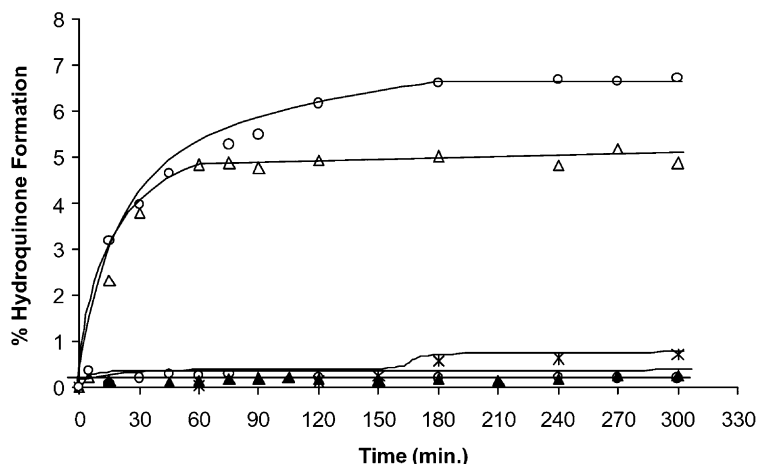


Fig. 5. The percentage of hydroquinone formation: [Fe(salpn)]-Y (○); [Cr(salpn)]-Y (△); [Bi(salpn)]-Y (\*); [Zn(salpn)]-Y (□) and [Ni(salpn)]-Y (▲).

of 3 h. A time of 1.5 h with 16% conversion of phenol was noted for [Cr(salpn)]-Y. Other catalysts recorded lower conversion than these two catalysts.

In terms of the formation of catechol and hydroquinone, a maximum of 16.5% catechol formation was obtained with iron based catalyst which was followed by chromium, bismuth, zinc and nickel based catalysts in decreasing order (Fig. 4). Similarly, hydroquinone formation of around 6.5% was obtained using iron based catalyst and this was followed by chromium, bismuth, zinc and nickel based catalysts (Fig. 5). The [Ni(salpn)]-Y has shown the poorest performance for the oxidation of phenol as well as the hydroquinone formation. The selectivities of two major products, catechol and hydroquinone were also found to be different from catalyst to catalyst. In spite of the low phenol conversion, the nickel and zinc based catalysts gave more than 92% selectivity for the catechol formation. The maximum percentage of selectivity of  $\sim 32$  for the hydroquinone formation was obtained with [Cr(salpn)]<sup>+</sup>-Y after 3 h of reaction time. This was followed by [Fe(salpn)]<sup>+</sup>-Y with 29% selectivity. Two more components with all the catalysts were also observed in the reaction mixture but in very small amounts (less than 0.5%) and no attempts were made to identify them. These are probably higher molecular weight compounds forming in the reaction mixture due to the association of catechol, as catechol has a tendency to polymerize.

#### 4. Conclusions

Physico-chemical studies present, clear evidence that encapsulation of metal complexes has occurred in the super cages ( $\alpha$ -cages) of Y-zeolite. These encapsulated complexes are active catalysts for the decomposition of hydrogen peroxide and for the oxidation of phenol to catechol and hydroquinone with good selectivity. The oxidation of phenol solely depends on the central metal ion present in the encapsulated complex and not on the H<sub>2</sub>O<sub>2</sub> decomposition ability of the catalyst. IR spectra of fresh and used catalyst are nearly identical with not much loss in intensity of the peaks, indicating that these catalysts can be used further for catalytic study.

#### Acknowledgements

SJJT thanks Indian Council for Cultural Relations (ICCR) for fellowship. The authors are thankful to Prof. S. Ray of Metallurgical and Materials Engineering Department, Indian Institute of Technology, Roorkee, for a fruitful discussion and the Head of the Department of Chemistry for necessary facilities.

#### References

- [1] R. Parton, D. De Vos, P.A. Jacobs, in: E.G. Derouane, F. Lemos, C. Naccache, F.R. Rebeiro (Eds.), Proceedings of



- the NATO Advanced Study Institute on Zeolite, Microporous Solid: Synthesis, Structure and Reactivity 555, Kluwer, Dodrecht, 1992, p. 578.
- [2] P.C.H. Mitchel, Chemistry and Industry, 6 May, (1991) 308.
- [3] C.R. Jacob, S.P. Varkey, P. Ratnasamy, Microporous and Mesoporous Materials 22 (1998) 465.
- [4] C.R. Jacob, S.P. Varkey, P. Ratnasamy, Appl. Catal. A General 168 (1998) 353.
- [5] S. Deshpande, D. Srinivas, P. Ratnasamy, J. Catal. 188 (1999) 261.
- [6] C. Bowers, P.K. Dutta, J. Catal. 122 (1990) 271.
- [7] P.-P. Knops-Gerrits, D.D. Vos, F. Thibaut-Starzk, P.A. Jacobs, Nature 369 (1994) 543.
- [8] D.D. Agrawal, R.P. Bhatnagar, R. Jain, S. Srivastava, J. Chem. Soc., Perkin. Trans. 2 (1990) 989.
- [9] S.P. Varkey, C.R. Jacob, Indian J. Chem. 37A (1998) 407.
- [10] C. Ratnasamy, A. Murugkar, S. Padhye, S.A. Pardhy, Indian J. Chem. 35A (1996) 1.
- [11] S. Kowalak, R.C. Weiss, K.J. Balkus, J. Chem. Soc., Chem. Commun. (1991) 57.
- [12] C.R. Jacob, S.P. Varkey, P. Ratnasamy, Appl. Catal. A General 182 (1999) 91.
- [13] M. Harimohan, F.L. Urbach, Inorg. Chem. 8 (1969) 556.
- [14] K.I. Balkus Jr., A.G. Gabrielov, Phenomena and molecular recognition in chemistry, J. Inclusion 21 (1995) 159.
- [15] F.A. Cotton, G. Wilkinson, Advance Inorganic Chemistry, 3rd Edition, Wiley Eastern, New Delhi, 1993, p. 838.
- [16] F.A. Cotton, G. Wilkinson, Advance Inorganic Chemistry, 3rd Edition, Wiley Eastern, New Delhi, 1993, p. 894.